Structural Engineering and Mechanics, Vol. 40, No. 3 (2011) 431-451
DOI: http://dx.doi.org/10.12989/sem.2011.40.3.431

Active control of a nonlinear and hysteretic building structure with time delay

Kun Liu, Long-Xiang Chen and Guo-Ping Cai*

Department of Engineering Mechanics, State Key Laboratory of Ocean Engineering, Shanghai Jiaotong University, Shanghai 200240, P.R. China

(Received December 1, 2010, Revised July 14, 2011, Accepted October 6, 2011)

Abstract. Time delay inevitably exists in active control systems, and it may cause the degradation of control efficiency or instability of the systems. So time delay needs to be compensated in control design in order to eliminate its negative effect on control efficiency. Today time delay in linear systems has been more studied and some treating methods had been worked out. However, there are few treating methods for time delay in nonlinear systems. In this paper, an active controller for a nonlinear and hysteretic building structure with time delay is studied. The nonlinear and hysteretic behavior of the system is illustrated by the Bouc-Wen model. By specific transformation and augmentation of state parameters, the motion equation of the system with explicit time delay is transformed into the standard state space representation without any explicit time delay. Then the fourth-order Runge-Kutta method and instantaneous optimal control method are applied to the controller design with time delay. Finally, numerical simulations and comparisons of an eight-story building using the proposed time-delay controller are carried out. Simulation results indicate that the control performance will deteriorate if time delay is not taken into account in the control design. The simulations also prove the proposed time delay controller in this paper can not only effectively compensate time delay to get better control effectiveness, but also work well with both small and large time delay problems.

Keywords: nonlinear and hysteretic building structure; active control; time delay

1. Introduction

During recent decades, time delay in structural vibration control has been a hot research topic. Various research results indicate that even a small time delay may cause actuators to apply energy to the control system when energy is actually not needed, which may cause degradation of control efficiency and even make the system unstable (Hu and Wang 2002, Cai *et al*. 2003, Chen 2009). Time delay has been also studied in many other research areas, such as information and communication technology, nonlinear dynamics etc, and is getting more and more attention.

So far some methods have been proposed to handle time delay problem in linear systems, such as Taylor series expansion (Abdel-Rohman 1987), phase shift technique (Chung *et al*. 1988), state pre-estimation (Greery *et al*. 1988) and two direct design methods for time-delay controller (Cai *et al*. 2003, Cai and Huang 2002). The first three methods work well with some small time delay

*Corresponding author, Professor, E-mail: caigp@sjtu.edu.cn

problems, but can not deal with large time delay ones. Two direct design methods (Cai *et al*. 2003, Cai and Huang 2002) are to design time-delay controller directly from time-delay differential equation and no assumption is made in the entire design process, and they are suitable for both small and large time delays. Chen (2009) and Chen *et al*. (2009) verified these two methods by experiment using several flexible structures as research objects. However, nonlinearity exists inevitably in practical engineering structures. Strictly speaking, all the structures in practice are nonlinear, and they can be grouped into weak nonlinear systems and strong nonlinear systems. Weak nonlinear systems could be changed into equivalent linear systems since the response caused by nonlinear factor of the structure is trivial, so the traditional linear system theory could be applied to the research of control of weak nonlinear systems, and the methods to handle time delay for linear systems could also be applicable for the time delay problem in weak nonlinear systems. Strong nonlinear systems, on the other hand, can not be equaled to linear ones because the response caused by nonlinear factor of the structure is significant. The linear system theory is not applicable for the analysis of strong nonlinear systems, and the nonlinear system theory should be considered. However, the nonlinear system theory scheme is not mature and there is not a universal analysis method applicable for all nonlinear systems up to now. Different nonlinear systems usually need different methods for the analysis.

Nowadays the time delay problem in nonlinear systems has come to many researchers' attention. For example, Ge *el al*. (2004) studied the adaptive neural control of a class of strict-feedback nonlinear systems with unknown time delays, Lyapunov-Krasovskii function is combined with the young's inequality to eliminate the unknown time delay in the upper bounding function of the Lyapunov functional derivative. Ge and Tee (2007) developed an approximation-based control method for multi-input/multi-output (MIMO) nonlinear systems with unknown state delays. By using Lyapunov-Krasovskii functions and adaptive neural network backstepping, the control method guarantees that all closed-loop signals remain bounded and the outputs converge to the proximity of the desired trajectories. Zhang *et al*. (2008) discussed the robust stability criteria for a class of uncertain neural systems with time-varying delays and nonlinear uncertainties, and by Lyapunov method, put forward a new delay-dependent stability criteria. Tian and Peng (2006), by Takagi-Sugeno fuzzy modeling and Lyapunov-Krasovskii functional method, worked on the delay-dependent stability and controller design of uncertain nonlinear time-varying delay systems, and suggested the sufficient conditions for stabilizing the uncertain systems. For the time delay problem in the controller design of nonlinear structures, to our knowledge, there are seldom any studies up to now.

This paper studies the active control of a nonlinear and hysteretic building structure with time delay and proposes a method to deal with the time delay. The proposed method works well with both small and large time delays. Numerical simulations prove the effectiveness of the proposed method. This paper is organized as follows. Section 2 briefly introduces nonlinear hysteretic model for inelastic systems, motion equation of the structural system with explicit time delay, and specific transformation and augmentation for standard state space representation without any explicit time delay. Instantaneous optimal controller design with time delay is given in Section 3, including the controller design and control implementation. Numerical simulations and comparisons of an eight-story building using the proposed time-delay controller are carried out in Section 4. Finally, concluding remarks are given in Section 5.

2. System nonlinear motion equation

2.1 Nonlinear hysteretic model for inelastic systems

Today, many hysteretic models have been developed to describe the restoring force of inelastic systems. In this paper, the Bouc-Wen model will be used for the structure. The stiffness restoring force based on the Bouc-Wen model can be written as (Ikhouane *et al*. 2007, Yang and Liu 1992)

$$F_{ki} = \alpha_i k_i x_i + (1-\alpha_i) k_i D_i v_i \tag{1}$$

where the subscript i represents the ith story unit; α_i is the ratio of postyielding with respect to preyielding stiffness; k_i represents the elastic stiffness; x_i is the interstory drift of the ith story unit; D_i is the yield constant displacement of the ith story unit; v_i is a nondimensional variable introduced to describe the hysteretic component of the deformation, with $|v_i| \le 1$, where

$$D_i \dot{v}_i = \bar{a}_i \dot{x}_i - \beta_i |\dot{x}_i| |v_i|^{\bar{n}_i - 1} v_i - \gamma_i \dot{x}_i |v_i|^{\bar{n}_i} \tag{2}$$

where $\bar{a}_i$, β_i and γ_i are parameters that describe the scale and general shape of the hysteresis loop and $\bar{n}_i$ is the parameter that describes the smoothness of the force-deformation curve.

2.2 Motion equation

Fig. 1 shows the structural model of an n-story building with a rubber bearing isolation system. The rubber bearing isolation system is connected by an active tuned mass damper (ATMD). The structure undergoes an one-dimensional earthquake ground acceleration $\ddot{X}_g(t)$.

Considering time delay $\bar{\lambda}$ in control, the motion equation of the structural system is written as

$$\mathbf{M}\ddot{\mathbf{X}}(t) + \mathbf{C}\dot{\mathbf{X}}(t) + \mathbf{F}_k[\mathbf{X}(t)] = -\mathbf{M}_0 \ddot{X}_g(t) + \mathbf{H}\bar{U}(t-\bar{\lambda}) \tag{3}$$

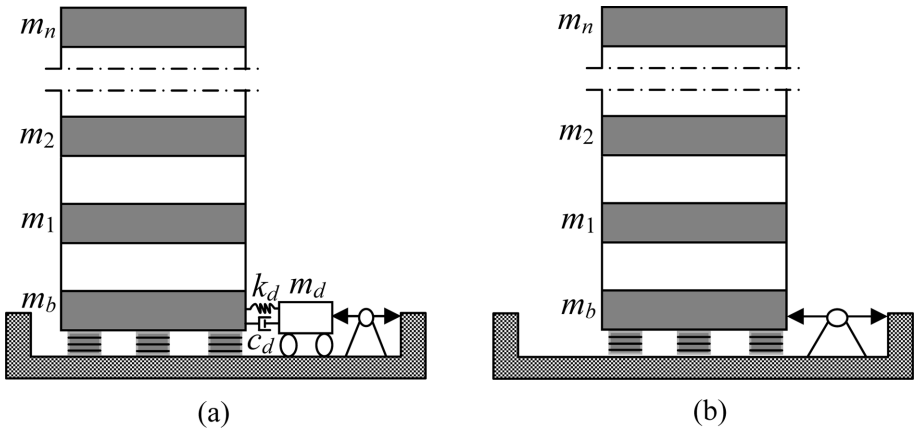

Fig. 1 Structural model of an n-story building equipped with a rubber bearing isolation system and (a) an active tuned mass damper (ATMD), (b) an actuator

where $X = [x_d, x_b, x_1, \ldots, x_n]^T$ is an $(n+2)\times 1$ vector of interstory drift, x_d and x_b are the interstory drift of ATMD and of rubber bearing isolation system, respectively, $x_1, \ldots, x_n$ are the interstory drift of each story unit of upper building structure, repectively; n is the degree of freedom of upper building structure. The parameter $\mathbf{M}$ is an $(n+2)\times(n+2)$ mass matrix, all elements of $\mathbf{M}$ are zero except $\mathbf{M}(1,1) = m_d$, $\mathbf{M}(2,2) = m_b$ and $\mathbf{M}(p,s) = m_{p-2}$ for $p = 3, \ldots, (n+2)$ and $s = 2, \ldots, p$. The parameter $\mathbf{C}$ is an $(n+2)\times(n+2)$ damping matrix, all elements of $\mathbf{C}$ are zero except $\mathbf{C}(1,1) = -\mathbf{C}(1,2) = \mathbf{C}(2,1) = c_d$, $\mathbf{C}(2,2) = c_d + c_b$, $\mathbf{C}(p,p) = c_{p-2}$ for $p = 3, \ldots, (n+2)$ and $\mathbf{C}(p,p+1) = -c_{p-1}$ for $p = 2, \ldots, (n+1)$. The parameter $\mathbf{M}_0$ is an $(n+2)\times 1$ vector whose elements are the mass of each story unit. $\mathbf{H}$ is an $(n+2)\times 1$ vector denoting the location of the active control force; $\overline{U}(t-\overline{\lambda})$ is the active control force. $\mathbf{F}_x[\mathbf{X}(t)]$ in Eq. (3) is the restoring force matrix, it can be written as

$$\mathbf{F}_k[\mathbf{X}(t)] = \mathbf{K}_1\mathbf{X}(t) + \mathbf{K}_2\mathbf{V}(t) \tag{4}$$

where $\mathbf{K}_1$ is an $(n+2)\times(n+2)$ elastic stiffness matrix, all elements of $\mathbf{K}_1$ are zero except $\mathbf{K}_1(1,1) = -\mathbf{K}_1(1,2) = -\mathbf{K}_1(2,1) = k_d$, $\mathbf{K}_1(2,2) = k_d + \alpha_b k_b$, $\mathbf{K}_1(p,p) = k_{p-2}$, for $p = 3, \ldots, (n+2)$ and $\mathbf{K}_1(p,p+1) = -k_{p-1}$ for $p = 2, \ldots, (n+1)$; $\mathbf{K}_2$ is an $(n+2)\times(n+2)$ hysteretic stiffness matrix, all elements of $\mathbf{K}_2$ are zero except $\mathbf{K}_2(2,2) = (1-\alpha_b)k_b D_b$; α_b is the ratio of postyielding stiffness with respect to preyielding stiffness of the rubber bearing isolation system; D_b is the yield constant displacement of the rubber bearing isolation system; $\mathbf{V}$ is an $(n+2)\times 1$ vector denoting the hysteretic variable of each story unit, $\mathbf{V} = [v_d, v_b, v_1, \ldots, v_n]^T$. According to Eq. (2), $\mathbf{V}$ can be described as follows

$$\dot{\mathbf{V}} = \mathbf{f}(\dot{\mathbf{X}}, \mathbf{V}) \tag{5}$$

The ith element of $\dot{\mathbf{V}}$ can be written as

$$\dot{v}_i = f(\dot{x}_i, v_i) = D_i^{-1}(\overline{a}_i\dot{x}_i - \beta_i|\dot{x}_i||v_i|^{\overline{n}_i - 1}v_i - \gamma_i\dot{x}_i|v_i|^{\overline{n}_i}) \tag{6}$$

It should be noted that for the control system consisting of either only a rubber bearing isolation system or a rubber bearing isolation system plus an actuator, matrices in motion Eq. (3) should be modified accordingly.

In the state space representation, Eq. (3) becomes

$$\dot{\mathbf{Z}}(t) = \mathbf{A}\mathbf{Z}(t) + \mathbf{W}\ddot{X}_g(t) + \mathbf{B}\overline{U}(t-\overline{\lambda}) + \mathbf{B}_1\mathbf{V}(t) \tag{7}$$

where

$$\mathbf{Z}(t) = \begin{bmatrix}\mathbf{X}(t)\\ \dot{\mathbf{X}}(t)\end{bmatrix},\ \mathbf{A} = \begin{bmatrix}\mathbf{0} & \mathbf{I}\\ -\mathbf{M}^{-1}\mathbf{K}_1 & -\mathbf{M}^{-1}\mathbf{C}\end{bmatrix},\ \mathbf{W} = \begin{bmatrix}\mathbf{0}\\ -\mathbf{M}^{-1}\mathbf{M}_0\end{bmatrix},\ \mathbf{B} = \begin{bmatrix}\mathbf{0}\\ \mathbf{M}^{-1}\mathbf{H}\end{bmatrix},$$

$$\mathbf{B}_1 = \begin{bmatrix}\mathbf{0}\\ -\mathbf{M}^{-1}\mathbf{K}_2\end{bmatrix}$$

By the following transformation of Eq. (7) (Cai and Huang 2003)

$$\begin{aligned}\overline{\mathbf{H}}(t) &= \mathbf{Z}(t) + \mathbf{\Gamma}(t) \\ &= \mathbf{Z}(t) + \int_{-\bar{\lambda}}^{0} e^{-\mathbf{A}(\eta+\bar{\lambda})}\mathbf{B}\overline{\mathbf{U}}(t+\eta)d\eta\end{aligned} \tag{8}$$

then Eq. (7) becomes

$$\dot{\overline{\mathbf{H}}}(t) = \mathbf{A}\overline{\mathbf{H}}(t) + \mathbf{W}\ddot{X}_g(t) + \overline{\mathbf{B}}\overline{U}(t) + \mathbf{B}_1\mathbf{V}(t) \tag{9}$$

where $\overline{\mathbf{B}} = e^{-\mathbf{A}\bar{\lambda}}\mathbf{B}$.

Augmenting the state variables in Eq. (9) and defining a new state vector as $\tilde{\mathbf{H}}(t) = \begin{bmatrix}\overline{\mathbf{H}} \\ \mathbf{V}\end{bmatrix}$, Eq. (9) then can be expressed as follows

$$\dot{\tilde{\mathbf{H}}}(t) = \mathbf{g}'[\tilde{\mathbf{H}}(t)] + \tilde{\mathbf{W}}\ddot{X}_g(t) + \tilde{\mathbf{B}}\overline{U}(t) \tag{10}$$

where $\tilde{\mathbf{W}} = \begin{bmatrix}\mathbf{W} \\ \mathbf{0}\end{bmatrix}$ and $\tilde{\mathbf{B}} = \begin{bmatrix}\overline{\mathbf{B}} \\ \mathbf{0}\end{bmatrix}$. $\mathbf{g}'[\tilde{\mathbf{H}}(t)]$ can be written as

$$\mathbf{g}'[\tilde{\mathbf{H}}(t)] = \begin{bmatrix}\mathbf{A}\overline{\mathbf{H}} + \mathbf{B}_1\mathbf{V} \\ \mathbf{f}(\dot{\mathbf{X}}, \mathbf{V})\end{bmatrix} \tag{11}$$

Thus, by the transformation and augmentation described above, Eq. (7) changes to Eq. (10) in the state space representation without any explicit time delay, which can be solved numerically step by step using the fourth-order Runge-Kutta method. The algorithm is described as follows

$$\tilde{\mathbf{H}}(t) = \tilde{\mathbf{H}}(t - 2\Delta t) + \frac{1}{6}(\mathbf{A}_0 + 2\mathbf{A}_1 + 2\mathbf{A}_2 + \mathbf{A}_3) \tag{12}$$

where Δt is the integration step of time; $\mathbf{A}_0$, $\mathbf{A}_1$, $\mathbf{A}_2$ and $\mathbf{A}_3$ can be written as

$$\begin{cases}\mathbf{A}_0 = 2\Delta t\{\mathbf{g}'[\tilde{\mathbf{H}}(t - 2\Delta t)] + \tilde{\mathbf{B}}\overline{U}(t - 2\Delta t) + \tilde{\mathbf{W}}\ddot{X}_g(t - 2\Delta t)\} \\ \mathbf{A}_1 = 2\Delta t\{\mathbf{g}'[\tilde{\mathbf{H}}(t - 2\Delta t) + 0.5\mathbf{A}_0] + \tilde{\mathbf{B}}\overline{U}(t - \Delta t) + \tilde{\mathbf{W}}\ddot{X}_g(t - \Delta t)\} \\ \mathbf{A}_2 = 2\Delta t\{\mathbf{g}'[\tilde{\mathbf{H}}(t - 2\Delta t) + 0.5\mathbf{A}_1] + \tilde{\mathbf{B}}\overline{U}(t - \Delta t) + \tilde{\mathbf{W}}\ddot{X}_g(t - \Delta t)\} \\ \mathbf{A}_3 = 2\Delta t\{\mathbf{g}'[\tilde{\mathbf{H}}(t - 2\Delta t) + \mathbf{A}_2] + \tilde{\mathbf{B}}\overline{U}(t) + \tilde{\mathbf{W}}\ddot{X}_g(t)\}\end{cases} \tag{13}$$

Substituting Eq. (13) into Eq. (12), one can obtain

$$\tilde{\mathbf{H}}(t) = \overline{\mathbf{D}}(t - 2\Delta t,\ \ t - \Delta t) + \frac{\Delta t}{3}[\tilde{\mathbf{B}}\overline{U}(t) + \tilde{\mathbf{W}}\ddot{X}_g(t)] \tag{14}$$

where

$$\begin{aligned}\overline{\mathbf{D}}(t-2\Delta t,\ \ t-\Delta t) = \tilde{\mathbf{H}}(t-2\Delta t) + \frac{1}{3}\Delta t\{\mathbf{g}'[\tilde{\mathbf{H}}(t-2\Delta t)] + \tilde{\mathbf{B}}\overline{U}(t-2\Delta t) + \\ \tilde{\mathbf{W}}\ddot{X}_g(t-2\Delta t) + 2\mathbf{g}'[\tilde{\mathbf{H}}(t-2\Delta t) + 0.5\mathbf{A}_0] + 4\tilde{\mathbf{B}}\overline{U}(t-\Delta t) + \\ 4\tilde{\mathbf{W}}\ddot{X}_g(t-\Delta t) + 2\mathbf{g}'[\tilde{\mathbf{H}}(t-2\Delta t) + 0.5\mathbf{A}_1] + \mathbf{g}'[\tilde{\mathbf{H}}(t-2\Delta t) + \mathbf{A}_2]\}\end{aligned} \tag{15}$$

3. Instantaneous optimal control

In last section, the motion equation of the structural system is changed into the state space representation without any explicit time delay by specific transformation and augmentation. In this section, the instantaneous optimal control method, proposed by Yang and Liu (1992), is applied for the control of the above-mentioned hysteretic system with time delay.

3.1 Design of controller

The time dependent quadratic objective function $J(t)$ can be describe as follows (Yang and Liu 1992)

$$J(t) = \tilde{\mathbf{H}}^T(t)\mathbf{Q}\tilde{\mathbf{H}}(t) + \bar{U}^T(t)R\bar{U}(t) \tag{16}$$

where $\mathbf{Q}$ is non-negative definite symmetric matrix and R is a positive constant. Now the task is to design an optimal controller for the hysteretic system by minimizing the objective function $J(t)$ subjected to the constraint given by Eq. (14) at every time instant t.

The Hamiltonian Y is constructed by introducing a $(3n+6)$-dimensional Lagrangian multiplier vector $\boldsymbol{\lambda}(t)$

$$\begin{aligned} Y &= \tilde{\mathbf{H}}^T(t)\mathbf{Q}\tilde{\mathbf{H}}(t) + \bar{U}^T(t)R\bar{U}(t) \\ &+ \boldsymbol{\lambda}^T(t)\{\tilde{\mathbf{H}}(t) - \bar{\mathbf{D}}(t-2\Delta t,\ t-\Delta t) - \frac{\Delta t}{3}[\tilde{\mathbf{B}}\bar{U}(t) + \tilde{\mathbf{W}}\ddot{X}_g(t)]\} \end{aligned} \tag{17}$$

The necessary conditions for minimizing the objective function $J(t)$ subjected to the constraint given by Eq. (14) can be written as

$$\begin{cases} \dfrac{\partial Y}{\partial \tilde{\mathbf{H}}(t)} = \mathbf{0} \\ \dfrac{\partial Y}{\partial \bar{U}(t)} = 0 \\ \dfrac{\partial Y}{\partial \boldsymbol{\lambda}(t)} = \mathbf{0} \end{cases} \tag{18}$$

Substituting Eq. (17) into the first two expressions of Eq. (18), we have

$$\begin{cases} 2\mathbf{Q}\tilde{\mathbf{H}}(t) + \boldsymbol{\lambda}(t) = \mathbf{0} \\ 2R\bar{U}(t) - \dfrac{\Delta t}{3}\tilde{\mathbf{B}}^T\boldsymbol{\lambda}(t) = 0 \end{cases} \tag{19}$$

From Eq. (19), the expression of optimal controller can be described as follows

$$\bar{U}(t) = -\frac{\Delta t}{3}R^{-1}\tilde{\mathbf{B}}^T\mathbf{Q}\tilde{\mathbf{H}}(t) \tag{20}$$

It is observed from Eqs. (10) and (8) that, $\tilde{\mathbf{H}}(t)$ in Eq. (20) is composed of $\overline{\mathbf{H}}(t)$ and $\mathbf{V}(t)$, and $\overline{\mathbf{H}}(t)$ contains the integral term $\boldsymbol{\Gamma}(t) = \int_{-\bar{\lambda}}^{0} e^{-\mathbf{A}(\eta+\bar{\lambda})}\mathbf{B}\bar{\mathbf{U}}(t+\eta)d\eta$.

From Eqs. (14) and (20), when there is no time delay in the system, namely $\overline{\lambda} = 0$, the controller $\overline{U}(t)$ at time instant t depends on the following parameters: the external excitation at time instant t; the controller and the external excitation at time instant $(t-\Delta t)$; the state vector, the controller and the external excitation at time instant $(t-2\Delta t)$. When time delay exists in the system, namely $\overline{\lambda} \neq 0$, the controller $\overline{U}(t)$ at time instant t is not only related to those mentioned above, but also to the integral term $\Gamma(t)$ in Eq. (8). The computing of this integral term is given below.

3.2 Control Implementation

The data sampling period $\overline{T}$ is chosen to be identical with the computing time step Δt, i.e., $\overline{T} = \Delta t$. Assuming that time delay can be written as

$$\overline{\lambda} = l\overline{T} - \overline{m} \tag{21}$$

where l is a positive integral number, $l > 0$, $0 \leq \overline{m} < \overline{T}$. It is pointed out in (Sun 1989) that time delay has small effect on control performance and can be ignored in control design if time delay is smaller than data sampling period $\overline{T}$, time delay affects control system only when it is larger than $\overline{T}$. So this paper only considers the situation of $\overline{\lambda} > \overline{T}$ with the condition of $\overline{m} = 0$, i.e., time delay is integer times of sampling period. For the case of $\overline{m} \neq 0$, refer to (Cai and Huang 2002, Sun 1989).

Between any two adjoining sampling points, the control force exerted on the structure can be considered as a constant if the data sampling period is small enough, that is

$$\overline{U}(t) = \overline{U}(\overline{k}\overline{T}), \quad \overline{k}\overline{T} \leq t < (\overline{k}+1)\overline{T} \tag{22}$$

Since numerical computation for the control system is carried out on every sampling point only, when $\overline{m} = 0$, the integral term $\Gamma(t)$ in Eq. (8) can be written as (Cai and Huang 2003)

$$\begin{aligned} \mathbf{\Gamma}(t) = {} & \mathbf{IG}(\Delta t)\overline{U}(t - l\Delta t) + \mathbf{F}(-\Delta t)\mathbf{G}(\Delta t)\overline{U}[t - (l-1)\Delta t] \\ & + \mathbf{F}(-2\Delta t)\mathbf{G}(\Delta t)\overline{U}[t - (l-2)\Delta t] \\ & + \cdots + \mathbf{F}[-(l-1)\Delta t]\mathbf{G}(\Delta t)\overline{U}(t - \Delta t) \end{aligned} \tag{23}$$

where

$$\begin{cases} \mathbf{F}(\overline{\xi}) = e^{\mathbf{A}\overline{\xi}} \\ \mathbf{G}(\overline{\xi}) = \int_0^{\overline{\xi}} e^{-\mathbf{A}\theta} d\theta \cdot \mathbf{B} \end{cases} \tag{24}$$

We can observe from Eq. (23) that, when time delay exists in the system, every step of numerical computation for the controller given by Eq. (20), contains not only the state term of current step but also a linear combination of the former l steps of control.

$\mathbf{F}(\overline{\xi})$ and $\mathbf{G}(\overline{\xi})$ can be determined by the following equations (Cai and Huang 2002, Sun 1989)

$$\begin{cases} \mathbf{F}(\bar{\xi}) = e^{\mathbf{A}\bar{\xi}} = \sum_{j=0}^{\infty} \dfrac{\mathbf{A}^j \bar{\xi}^j}{j!} \\ \mathbf{G}(\bar{\xi}) = \int_0^{\bar{\xi}} e^{-\mathbf{A}\theta} d\theta \cdot \mathbf{B} = \sum_{j=1}^{\infty} \dfrac{(-\mathbf{A})^{j-1} \bar{\xi}^j}{j!} \cdot \mathbf{B} \end{cases} \tag{25}$$

When $\bar{\xi}$ is given, $\mathbf{F}(\bar{\xi})$ and $\mathbf{G}(\bar{\xi})$ will both converge to constant matrices in limited steps of iterative computation.

4. Numerical simulations

In order to verify the effectiveness of the mentioned optimal control method, numerical simulations are carried out in this section. An eight-story building adopted in (Yang and Liu 1992) is considered as the structural model. The Tianjin earthquake (in China) with a maximum ground acceleration of 0.4 g, as shown in Fig. 2, is used as the external excitation and the earthquake episode is 10 s.

The mass, elastic stiffness, damping coefficient and yield constant displacement of each story unit are shown in Table 1. Parameters of the hysteretic model are given as follows: $\alpha_i = 0.1$, $\bar{a}_i = 1.0$, $\beta_i = 0.5, \bar{n}_i = 95$ and $\gamma_i = 0.5$ for $i = 1 \sim 8$. The natural frequencies of the unyielded structure are 5.24, 14.0, 22.55, 30.22, 36.89, 43.06, 49.54 and 55.96 rad/s, respectively. The data sampling period

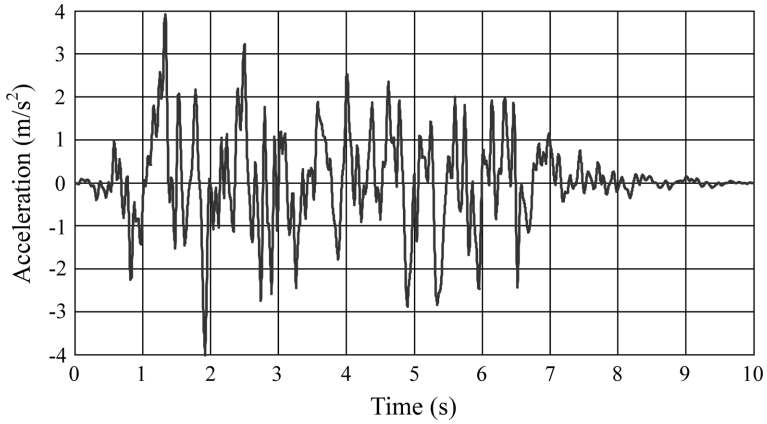

Fig. 2 Time history of the Tianjin earthquake

Table 1 The mass m_i, elastic stiffness k_i, damping coefficient c_i and yield constant displacement D_i of each story unit

Story	1	2	3	4	5	6	7	8
m_i (t)	345.6	345.6	345.6	345.6	345.6	345.6	345.6	345.6
k_i (10^5 kN/m)	3.4	3.26	2.85	2.69	2.43	2.07	1.69	1.37
c_i (kN s/m)	490	467	410	386	348	298	243	196
D_i (cm)	2.4	2.3	2.2	2.1	2.0	1.9	1.7	1.5

Table 2 maximum interstory drift x_i and maximum absolute acceleration a_i of each story unit
(x_i: cm, a_i: cm/s^2, D_i: cm)

Story (1)	D_i (2)	No control		With RBIS		ACTCON $\overline{U}_{max}$ = 692 kN		ATMDCON $\overline{U}_{max}$ = 224 kN	
		x_i (3)	a_i (4)	x_i (5)	a_i (6)	x_i (7)	a_i (8)	x_i (9)	a_i (10)
B	4	-	-	25.15	110	16.87	103	16.83	106
1	2.4	2.54	421	0.77	118	0.65	102	0.62	101
2	2.3	2.81	446	0.73	124	0.64	92	0.63	88
3	2.2	3.91	481	0.79	123	0.66	111	0.68	94
4	2.1	3.36	624	0.78	115	0.61	113	0.66	92
5	2.0	3.49	516	0.78	111	0.57	109	0.65	99
6	1.9	3.69	635	0.78	129	0.58	104	0.65	110
7	1.7	4.18	646	0.71	163	0.55	129	0.59	136
8	1.5	2.09	620	0.47	185	0.41	162	0.38	153

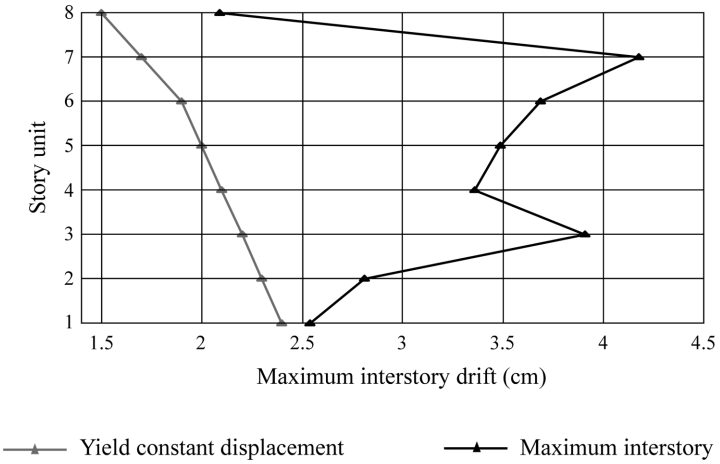

Fig. 3 Comparison of the yield constant displacement and the maximum interstory drift of each story unit without control

$\overline{T}$ and the computation time step Δt are both taken by 10^{-3} s, that is $\overline{T} = \Delta t = 10^{-3}$ s. The initial value of vectors **Z** and **V** are zero.

With the eight-story building structure described above and the Tianjin earthquake excitation shown in Fig. 2, the maximum interstory drift x_i and the maximum absolute acceleration a_i of each story unit without control are shown in columns 3 and 4 of Table 2. Fig. 3 shows the comparison of the yield constant displacement and the maximum interstory drift of each story unit without control. As observed from Table 2 and Fig. 3, for every story unit of the building structure without control, the deformation is excessive and yielding takes place in each story unit.

In order to reduce the structural response, a rubber bearing isolation system (RBIS) is implemented to the building structure, denoted by 'RBIS' in Table 3. The restoring force of the

Table 3 Three kinds of control strategies

RBIS	Rubber bearing isolation system only
ACTCON	Rubber bearing isolation system connected by an actuator
ATMDCON	Rubber bearing isolation system connected by an ATMD

RBIS is given in Eq. (1) with $i = b$. The mass, elastic stiffness and damping coefficient of the RBIS are $m_b = 450$ t, $k_b = 18050$ kN/m and $c_b = 26.17$ kN·s/m, respectively. The yield constant displacement and the ratio of postyielding stiffness with respect to preyielding stiffness of the RBIS are $D_b = 4$ cm and $\alpha_b = 0.6$, respectively. Parameters that describe the scale and general shape of the hysteresis loop of the RBIS are chosen as $\bar{a}_b = 1.0$, $\beta_b = 0.5$, $\bar{n}_b = 3$ and $\gamma_b = 0.5$. After adding the RBIS to the building structure, the natural frequencies of the entire building are 2.21, 9.31, 17.29, 25.18, 32.19, 38.29, 44.12, 50.37 and 56.74 rad/s, respectively.

The maximum responses of the building equipped with the RBIS are shown in columns 5 and 6 of Table 2. As observed from Table 2, the interstory drift and the absolute acceleration are evidently reduced. The interstory drift of each story unit of the upper structure is very small compared to that of the RBIS, and the upper structure tends to behave like a rigid body. However, as shown in column 5 of Table 2, the deformation of the RBIS may be excessive.

4.1 Optimal control with no time delay

In order to keep the safety and integrity of the RBIS, two measures are considered: (1) an actuator is connected to the RBIS as shown in Fig. 1(b), denoted by 'ACTCON' in Table 3; (2) an active tuned mass damper (ATMD) is connected to the RBIS as shown in Fig. 1(a), denoted by 'ATMDCON' in Table 3. Parameters of the ATMD are chosen as follows: The mass of the ATMD is $m_d = 172.8$ t; the natural frequency of the ATMD is chosen to be the same as the first natural frequency of the building with the rubber bearing isolation system, namely $\omega_d = 2.21$ rad/s; the damping ratio of the ATMD is $\xi_d = 10\%$, so the elastic stiffness and damping coefficient of the ATMD are $k_d = 844$ kN/m and $c_d = 76.38$ kN·s/m, respectively.

Firstly, we consider the case with no time delay in the control system, i.e., $\bar{\lambda} = 0$. The weighting matrix $\mathbf{Q}$ and scalar R in ACTCON and ATMDCON are chosen as follows

$$\text{ACTCON: } \begin{cases} \mathbf{Q} = \begin{bmatrix} \mathbf{Q}_{11} & \mathbf{0} & \mathbf{0} \\ \mathbf{0} & \mathbf{Q}_{22} & \mathbf{0} \\ \mathbf{0} & \mathbf{0} & \mathbf{0} \end{bmatrix}_{(3n+3)\times(3n+3)} \\ \mathbf{Q}_{11} = 1.42\times10^{6}\times\overline{\mathbf{T}}^{T}\mathbf{K}_1' \\ \mathbf{Q}_{22} = 1.42\times10^{6}\times\overline{\mathbf{T}}^{T}\mathbf{M}' \\ R = 0.0067 \end{cases} \tag{26}$$

where $n = 8$, $\mathbf{M}'$ and $\mathbf{K}_1'$ are $(n+1)\times(n+1)$ submatrices of $\mathbf{M}$ and $\mathbf{K}_1$, respectively, and they can be obtained by eliminating the first row and the first column of $\mathbf{M}$ and $\mathbf{K}_1$. $\overline{\mathbf{T}}$ is an $(n+1)\times(n+1)$ matrix, and all elements of $\overline{\mathbf{T}}$ are zero except $\overline{\mathbf{T}}(p,s) = 1$ for $p = 1,\ldots,(n+1)$ and $s = 1,2,\ldots,p$.

$$\text{ATMDCON: } \begin{cases} \mathbf{Q} = 402 \times \begin{bmatrix} \mathbf{0} & \mathbf{0} & \mathbf{0} \\ \mathbf{Q}_{21} & \mathbf{Q}_{22} & \mathbf{0} \\ \mathbf{0} & \mathbf{0} & \mathbf{0} \end{bmatrix}_{(3n+6)\times(3n+6)} \\ R = 5.025 \times 10^{-6} \end{cases} \tag{27}$$

where $n = 8$, $\mathbf{Q}_{21}$ and $\mathbf{Q}_{22}$ are $(n+2)\times(n+2)$ matrices. All elements of $\mathbf{Q}_{21}$ and $\mathbf{Q}_{22}$ are zero except $\mathbf{Q}_{21}(1,1) = 102$, $\mathbf{Q}_{21}(1,2) = -2363$, $\mathbf{Q}_{22}(1,1) = 67$, $\mathbf{Q}_{22}(1,2) = 731$.

Using the optimal controller with no time delay, the maximum interstory drift x_i and the maximum absolute acceleration a_i of each story unit with ACTCON and ATMDCON are shown in columns 7-10 of Table 2. The maximum active control forces with ACTCON and ATMDCON are also listed in Table 2. As observed from Table 2, after an actuator (ACTCON) or an ATMD (ATMDCON) being connected to the RBIS, the system is getting better control performance than with RBIS only. The deformations of the RBIS in ACTCON and ATMDCON are evidently reduced and the maximum response quantities of the upper building structure are further reduced than those in RBIS. It is also observed from Table 2 that the maximum responses of the building structure in ACTCON and ATMDCON are very close to each other, while the maximum active force in ATMDCON is much smaller than that in ACTCON. This is because the mass damper of ATMD in ATMDCON contributes to dissipate some energy generated by the strong earthquake, which explains the active control force generated by the actuator in ATMDCON is much smaller than that in ACTCON.

Figs. 4(a)-(c) show the results against time of the interstory drift and the absolute acceleration of the RBIS, the first story unit and the eighth story unit with ATMDCON, denoted by the solid line. The results of cases of no control, RBIS and ACTCON are also shown in Fig. 4 for comparison, and they are denoted by the dotted line, dashed line and dot-dashed line, respectively. Fig. 4(d) shows the active control force against time under ACTCON and ATMDCON.

4.2 Optimal control with time delay

Here we consider the case with time delay. Firstly, the effect of time delay on control performance is checked. Fig. 5 shows, against time delay, the maximum interstory drift and the maximum absolute acceleration of the RBIS and the first story unit, as well as the maximum active control forces under ACTCON and ATMDCON control. The results of the ACTCON and ATMDCON using the proposed time-delay controller are denoted by the dotted line and solid line in Fig. 5, respectively. For comparison, the results of the ACTCON and ATMDCON using the controller designed for the case with no time delay to control the system with time delay are also shown in Fig. 5, denoted by the dashed line and dot-dashed line, respectively. It is observed from Fig. 5 that the dashed line in ACTCON and dot-dashed line in ATMDCON appear to be in a rapid rise as time delay increases, which means that the control performance becomes worse and worse with the increase of time delay if time delay is neglected in control design. It is also observed that, when the proposed time-delay controller is used, the controlled structure still remains stable even when time delay increases to a relative large value. Furthermore, it is also observed from Fig. 5 that, when using the controller designed for the case with no time delay to control the system with time delay, the maximum responses in ATMDCON rise much slower than those that in ACTCON.

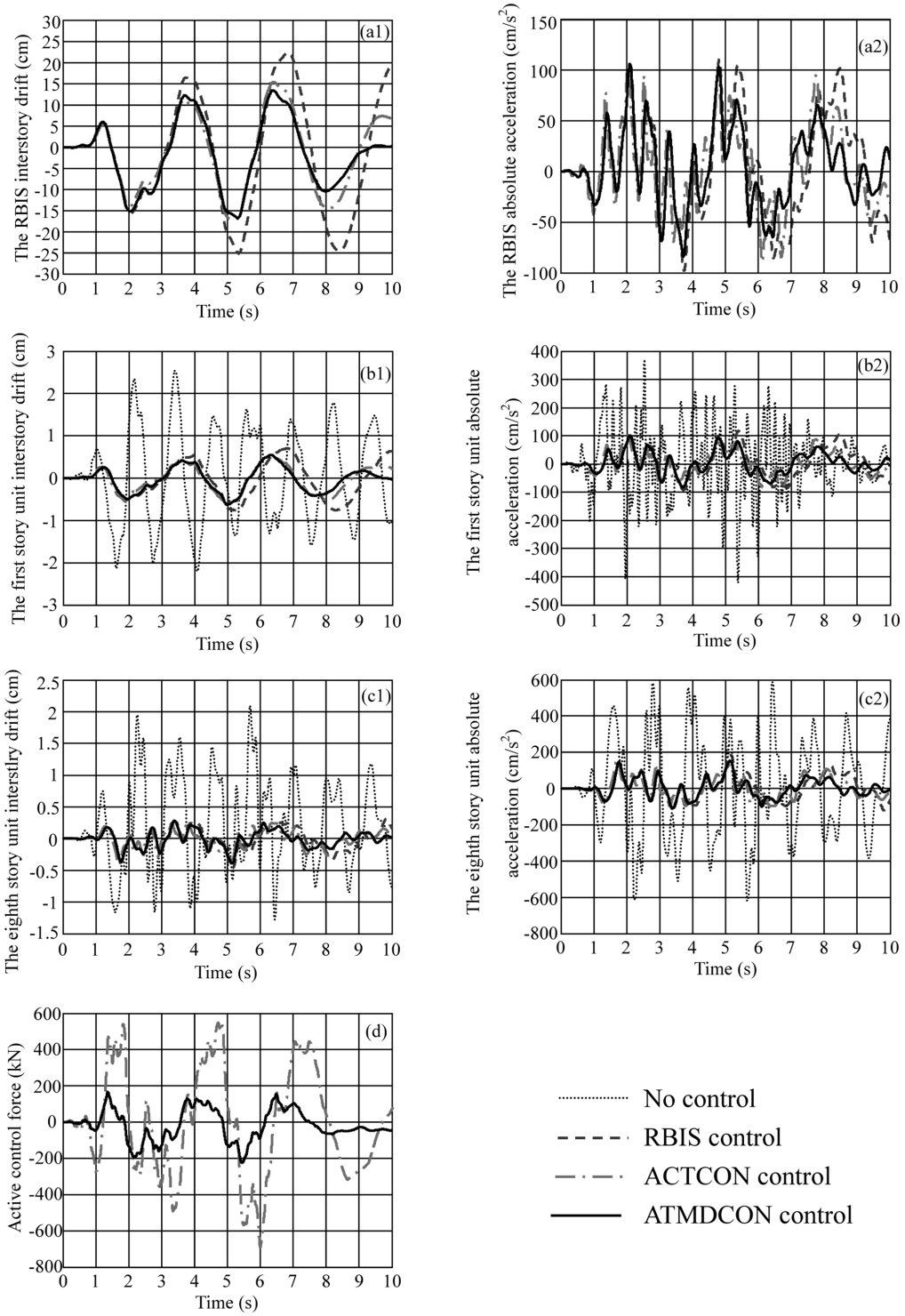

Fig. 4 Time histories of system response (a) the RBIS, (b) the first story unit, (c) the eighth story unit, (d) active control forces with ACTCON and ATMDCON

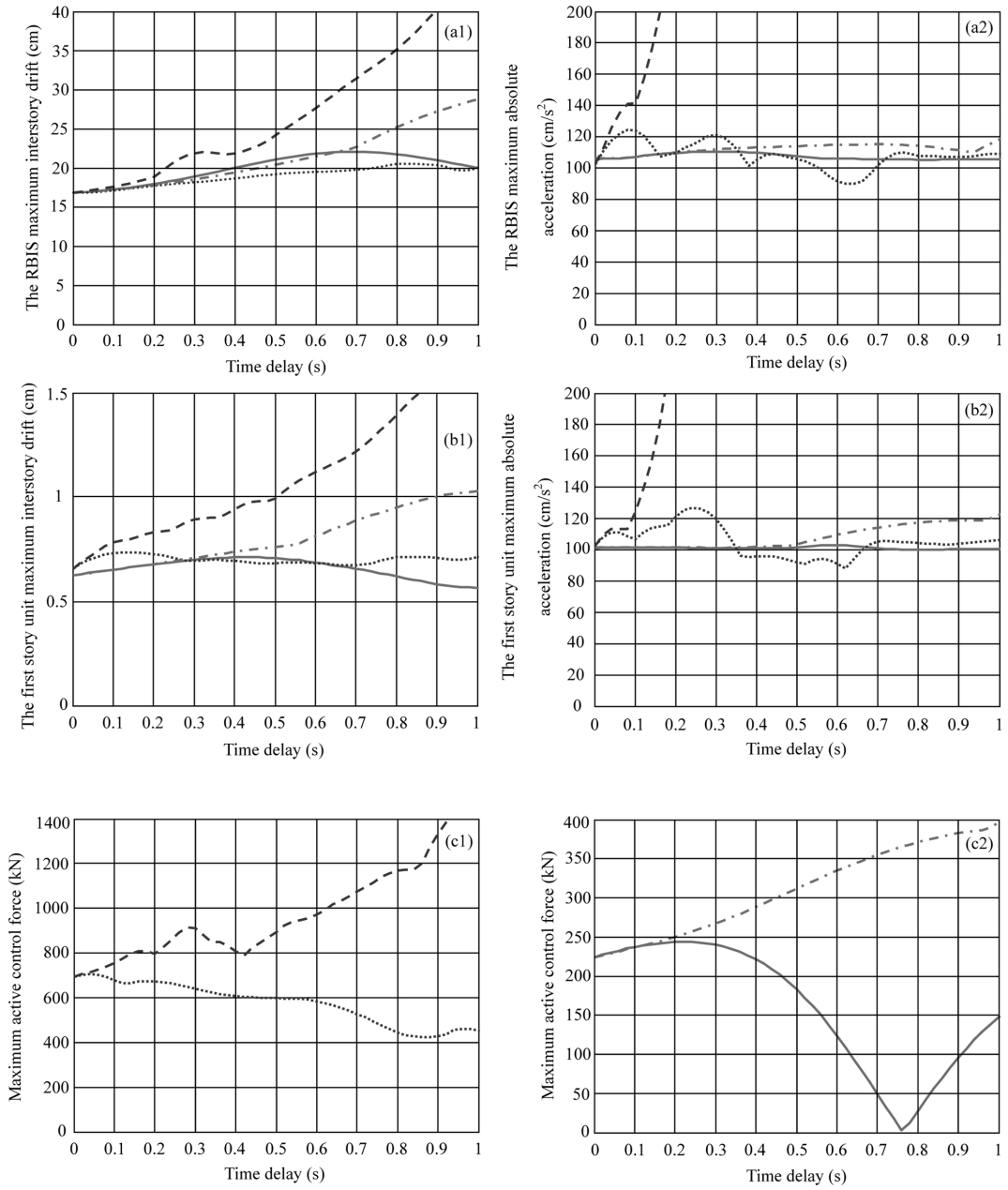

Fig. 5 The maximum response quantity and the maximum control force varying with time delay when using the controller with and without time delay to control the system with time delay (a) the RBIS, (b) the first story unit, (c) maximum active control force with ACTCON and ATMDCON

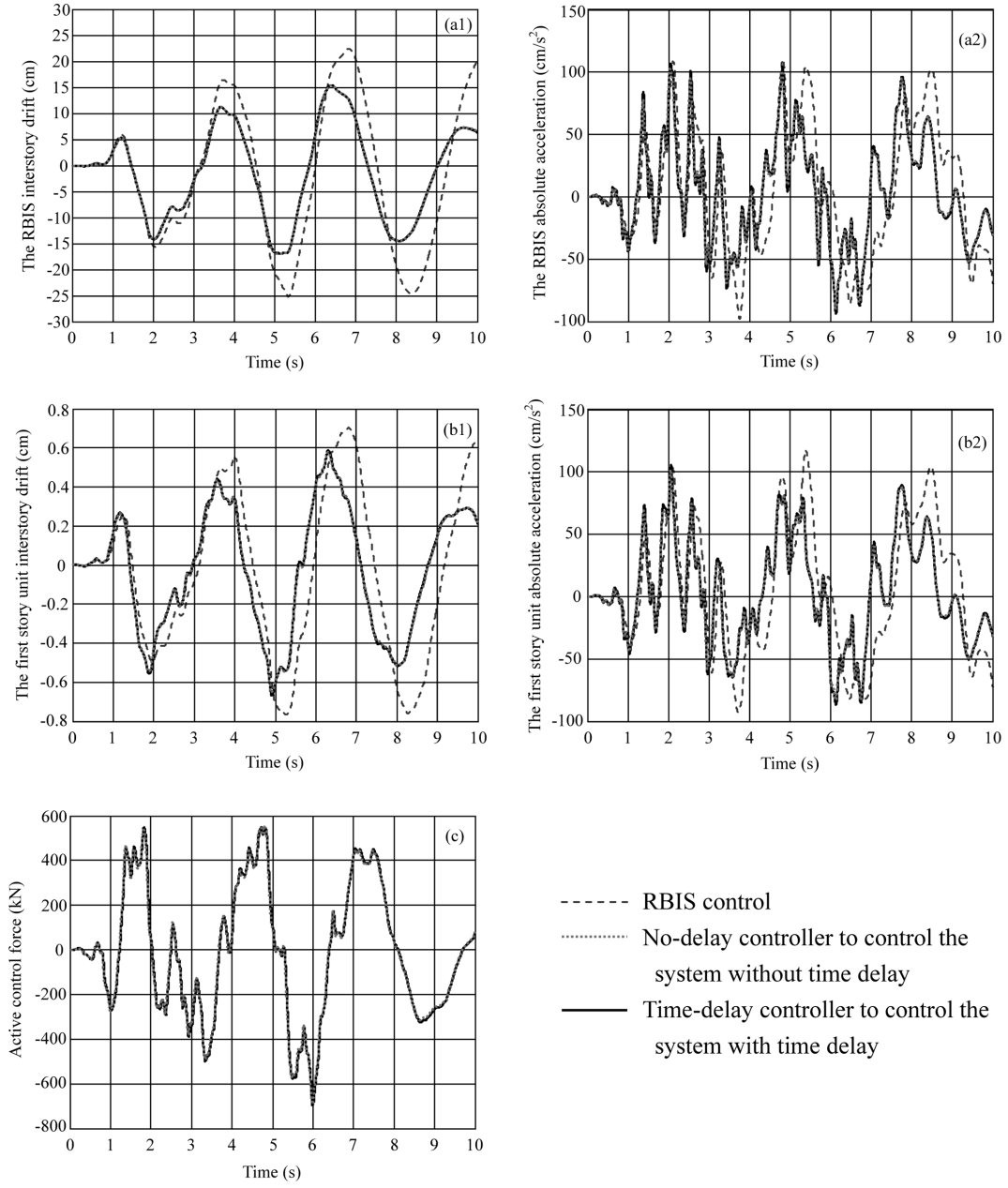

Fig. 6 Time histories of system response with ACTCON when time delay is 0.01 s (a) the RBIS, (b) the first story unit, (c) active control forces with ACTCON

Secondly, the effectiveness of the designed time-delay controller is verified. Two cases are considered: $\bar{\lambda} = 0.01$ s and $\bar{\lambda} = 0.6$ s. The results against time of the proposed time-delay controller are shown in Fig. 6 to Fig. 9. When $\bar{\lambda} = 0.01$ s, the interstory drift of the RBIS and the first story unit, the absolute acceleration of the RBIS and the first story unit, and the active control force, denoted by solid line are shown in Fig. 6 and Fig. 7, with respect to ACTCON and

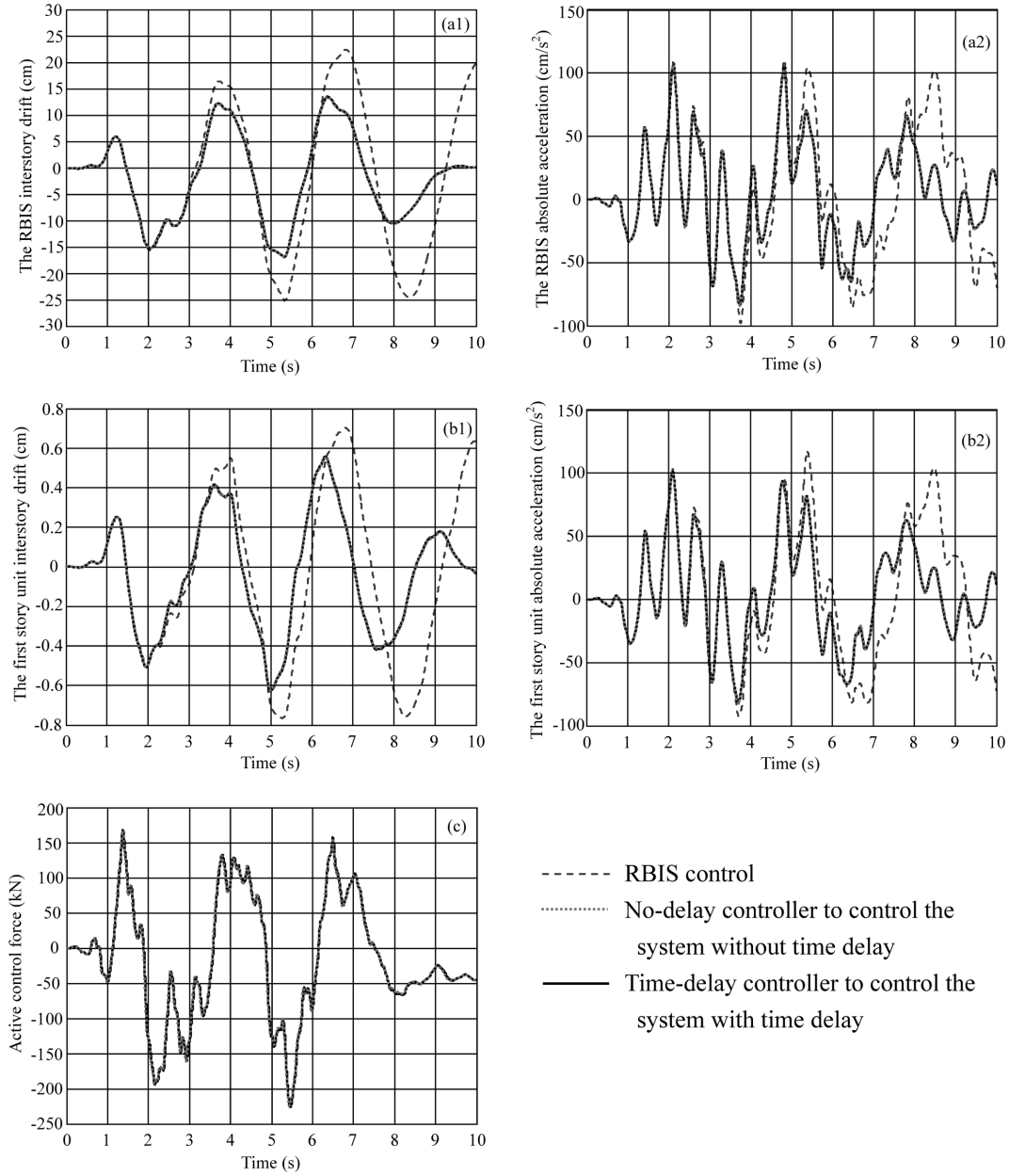

Fig. 7 Time histories of system response with ATMDCON when time delay is 0.01 s (a) the RBIS, (b) the first story unit, (c) active control forces with ATMDCON

ATMDCON accordingly. Figs. 8 and 9 are the same idea as Fig. 6 and Fig. 7 except for $\overline{\lambda} = 0.6$ s. The results of both the no-delay controller from Section 4.1 to control the system without time delay and the RBIS control are also shown in Figs. 6-9 for comparison purpose, which are denoted by dotted line and dashed line, respectively. It is observed from Figs. 6-9 that, for both ACTCON and ATMDCON, time delay is compensated effectively by the proposed time-delay controller and

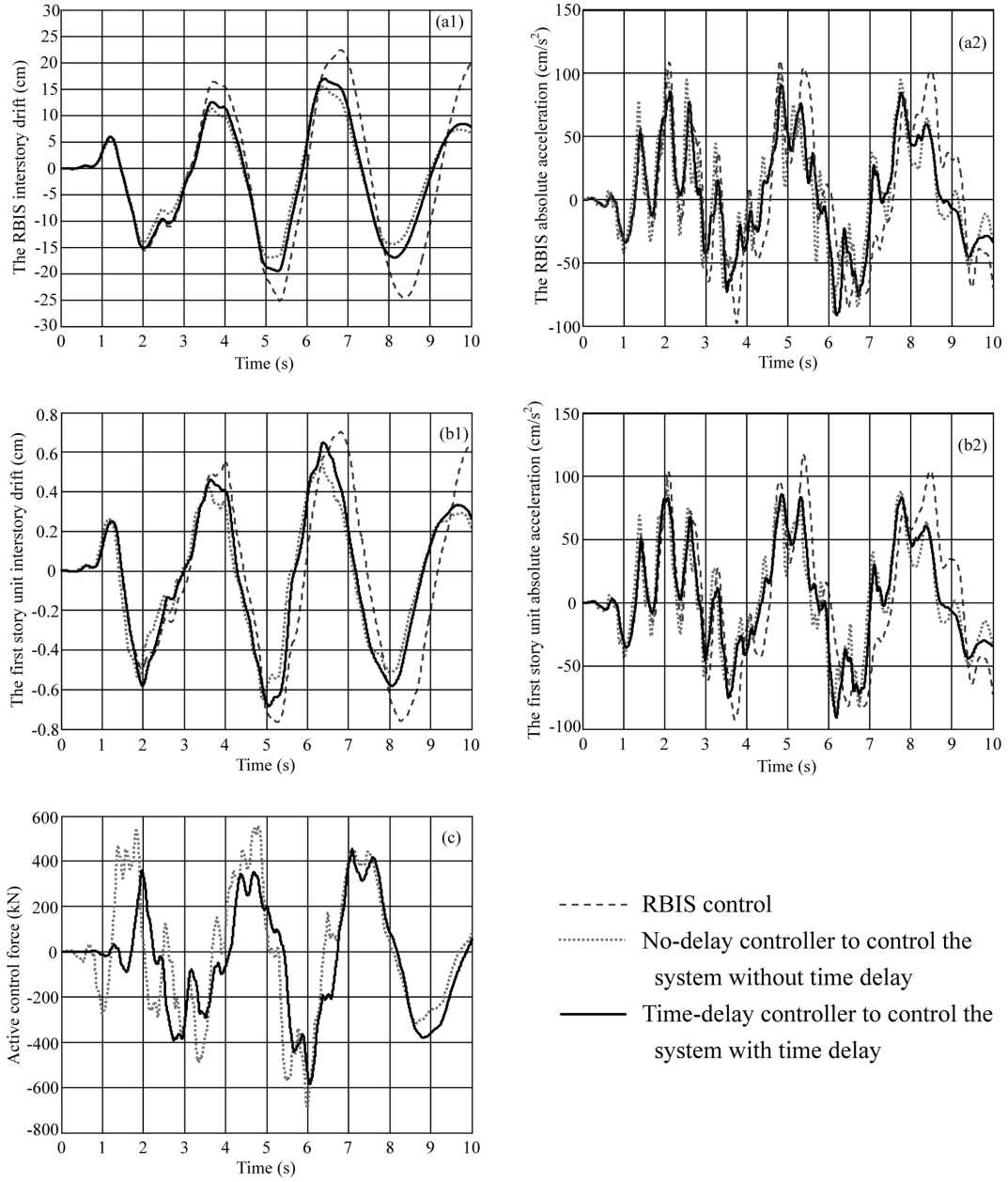

Fig. 8 Time histories of system response with ACTCON when time delay is 0.6 s (a) the RBIS, (b) the first story unit, (c) active control forces with ACTCON

excellent effectiveness can be obtained, which proves the proposed controller works well for both small and large time delay situations.

Our extensive simulation results indicate that the maximum responses of certain story units of the structure when using the time-delay controller are smaller than those when using the no-delay controller for some specific time delay, meanwhile the maximum active control force when using

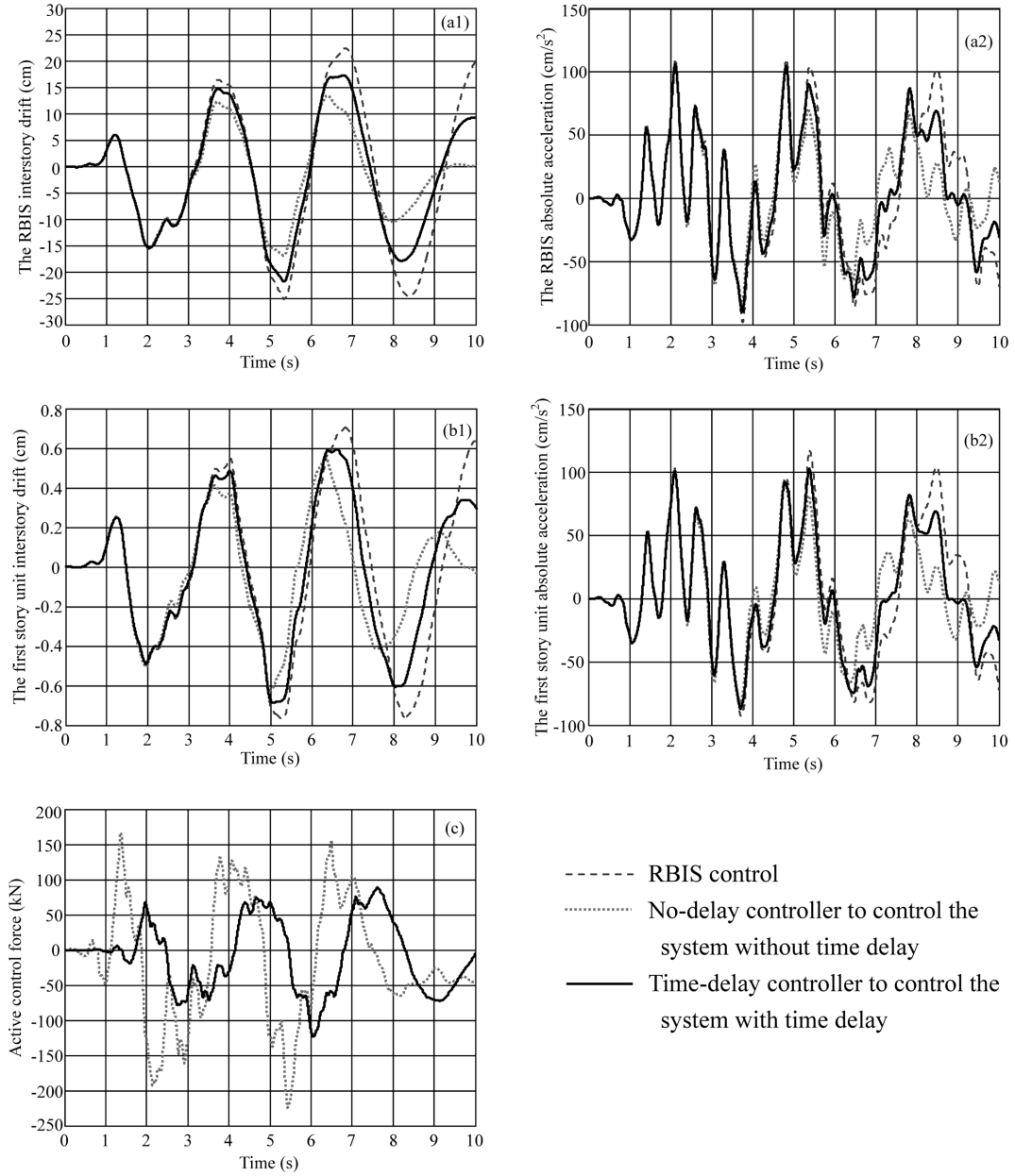

Fig. 9 Time histories of system response with ATMDCON when time delay is 0.6 s (a) the RBIS, (b) the first story unit, (c) active control forces with ATMDCON

the time-delay controller is also smaller than that when using the no-delay controller. Fig. 10 shows the maximum responses of the structure for $\overline{\lambda} = 0.6$ s under ACTCON and $\overline{\lambda} = 1$ s under ATMDCON, respectively. The maximum active control forces under ACTCON with no time delay and $\overline{\lambda} = 0.6$ s are 692 kN and 584 kN, respectively, and those that under ATMDCON with no time delay and $\overline{\lambda} = 1$ s are 224 kN and 148 kN. The results in Fig. 10 imply a possible utilization of

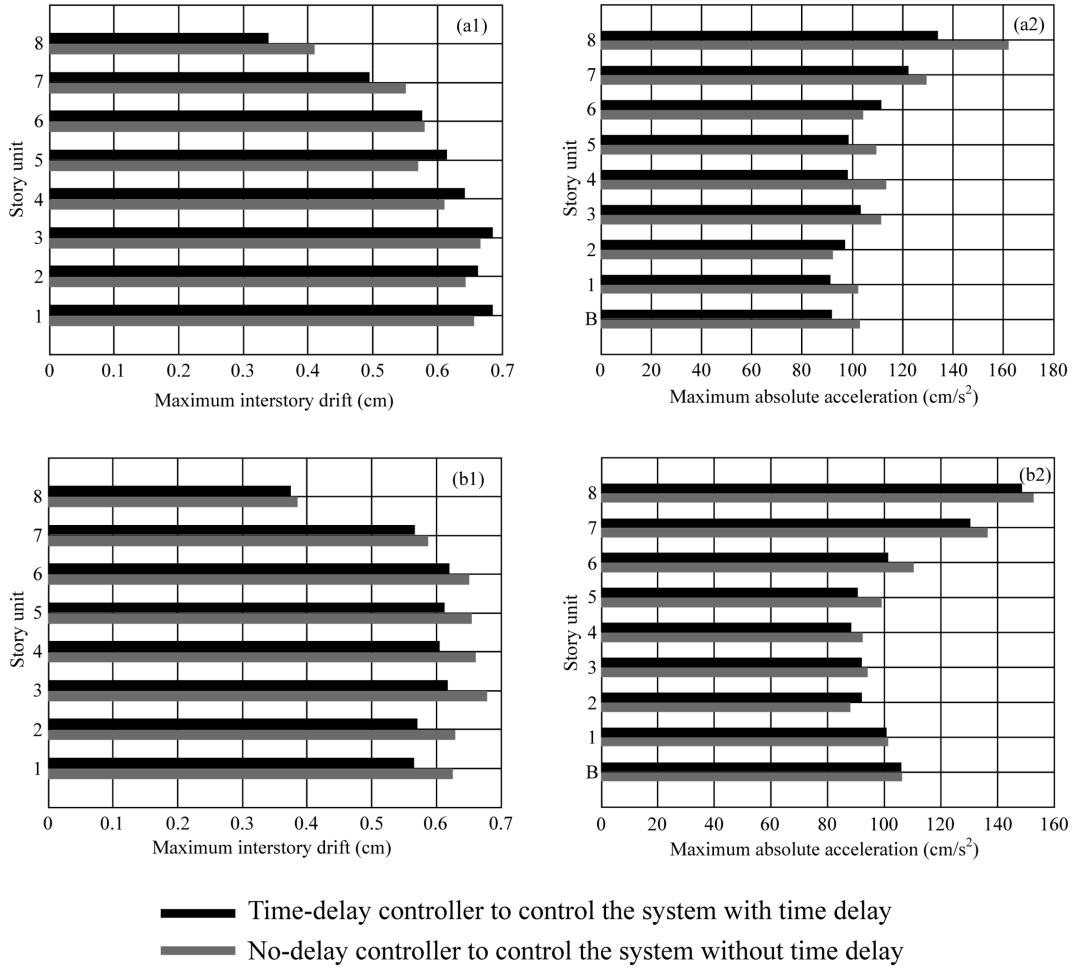

Fig. 10 Comparison of the maximum response quantity of each story unit when using the no-delay and time-delay controller (a) ACTCON control with $\overline{\lambda}$ = 0.6 s , (b) ATMDCON control with $\overline{\lambda}$ = 1 s

time delay for better control effectiveness. Even for a non-time-delay control system, a proper time delay for the system may be assumed and then a time-delay controller for better control effectiveness can be designed. Recent studies in some fields have shown that voluntary introduction of delays can also benefit the control. For example, in nonlinear dynamics area, achievement is remarkable when using time delay to control chaos motion (Ge *et al*. 2005, Xiao and Cao 2007). In structural control area, Hosek and Olgac (2002) developed a time-delay resonator that may be used for vibration control of structures. The main idea of time-delay resonator is to add a delayed feedback loop into control systems to reduce structural vibration by adjusting control weighting coefficient and the magnitude of time delay. In robotics area, Cai and Lim (2006) designed a time-delay controller for a flexible manipulator. Their results show that delayed feedback control design may possibly achieve much better control efficiency than the control design without time delay. In control system of pipeline transport, time delay may be utilized to enhance steady critical speed of flowing liquid (Yuan 2008). Time delay could be also used to improve system stability (Wang and

Hu 2006, Xu *et al*. 2007). Those researches above which involve the active utilization of time delay is so-called time-delay utilization technology or delayed feedback control method, which assumes time delay as a design parameter to obtain good control performance. Delayed feedback control is a novel control strategy and has been getting more and more attention. Many problems remain for extensive investigation.

Time-delay problems in the active structural control involve multiple disciplines like structure dynamics, control theory and mathematics. A sound solution to these problems is up to an effective synthesization of all these fields and will make significance to engineering applications. The authors believe more efforts should be put on the following areas.

(1) Time-delay identification: Current studies on time delay are almost all based on an assumption of a given/known certain amount of time delay, bypassing a very fundamental question of how much the delay is, that is how to identify the delay within the system. Time-delay identification is one of fundamentals of dynamic control and also the hardest part of the topic, especially when doing the experiment research. However, research on this topic makes theoretical importance with application potentials. Furthermore, when converting the problem of time-delay identification into the problem of optimization, the algorithm makes the most critical part. Current optimum-seeking algorithm turns out good within certain boundary conditions but fails to get a global optimal solution to the system. Although the stochastic optimization algorithm projects a brighter future, developing an algorism with higher efficiency and reliability still makes a topic which needs further study.

(2) Research on robust time-delay controller: In actual control system, the magnitude of time delay tends to be not significant, and might be varying within a limited range as well. Even for the control system with significant delay such as space-craft controller, the delay also appears to be in a small range. It surely will make a difference if a robust controller over time delay varying within a small range could be developed.

(3) Time-delay utilization: As stated in the above, current achievements on time delay show that the delay has some potential benefits. The utilization of time delay remains one of the important topics worth further study.

(4) Time-delay experiments: It means a lot to have more experiments on time delay to verify the theoretical results. However researches on experiments are very limited and theoretical results are always obtained under some ideal premises and not all the factors are taken into account, which means the theoretical results might not reflect in actual tests. As shown in (Cai and Lim 2006), the more the time delay, the better the control effectiveness, however this prediction does not prove in our experiment (Chen 2009, Chen *et al*. 2009).

(5) In recent years, the research achievements on time delay in the area of automation are worth attention, such as time-delay filter which can filter out the exponentially decaying sine vibrating signals; time-delay observer which can observe the uncertainty and external disturbance of the system and thus to get the robust control of the system; time-delay learning controller which can be used to non-differentially track the arbitrary periodic signals. How to apply above achievements to the actual control of flexible structures deserves further exploration.

5. Conclusions

By using the instantaneous optimal control method, this paper studies the aseismic active control

of a nonlinear and hysteretic building structure with time delay. The Bouc-Wen hysteretic model is applied to describe the stiffness restoring force of the nonlinear and inelastic structural system. The hysteretic components of the system are included in the motion equation to design the optimal time-delay controller. Simulation results indicate that, when no time delay exists in the control system, optimal controller can effectively reduce the responses of the building structure. When time delay exists, the control performance becomes worse if time delay is not compensated in control design. The time-delay controller proposed in this paper can effectively deal with the time delay in the system, and is applicable for both small and large time delay problems.

Acknowledgements

This work was supported by the Key Project [grant number 11132001] and the General Projects [grant numbers 11072146, 11002087] of Natural Science Foundation of China.

References

Abdel-Rohman, M. (1987), "Time-delay effects on active damped structures", *J. Eng. Mech.-ASCE*, **113**(11), 1709-1719.

Cai, G.P. and Huang, J.Z. (2002), "Optimal control method for seismically excited building structures with time-delay in control", *J. Eng. Mech.-ASCE*, **128**(6), 602-612.

Cai, G.P. and Huang, J.Z. (2003), "Instantaneous optimal method for vibration control of linear sampled-data systems with time delay in control", *J. Sound Vib.*, **262**, 1057-1071.

Cai, G.P., Huang, J.Z. and Yang, S.X. (2003), "An optimal control method for linear systems with time delay", *Comput. Struct.*, **81**(15), 1539-1546.

Cai, G.P. and Lim, C.W. (2006), "Optimal tracking control of flexible hub-beam system with time delay", *Multibody Syst. Dyn.*, **16**(4), 331-350.

Chen, L.X. (2009), "Delayed feedback control and experiment study of flexible structures", Ph.D. Thesis, Shanghai Jiaotong University, Shanghai. (in Chinese)

Chen, L.X., Cai, G.P. and Pan, J. (2009), "Experimental study of delayed feedback control for a flexible plate", *J. Sound Vib.*, **322**(4-5), 629-651.

Chung, L.L., Reinhorn, A.M. and Soong, T.T. (1988), "Experiments on active control of seismic structures", *J. Eng. Mech.-ASCE*, **114**(2), 241-256.

Ge, S.S., Hong, F. and Lee, T.H. (2004), "Adaptive neural control of nonlinear time-delay system with unknown virtual control coefficients", *IEEE T. Syst. Man Cy. B.,* **34**(1), 499-516.

Ge, S.S. and Tee, P.P. (2007), "Approximation-based control of nonlinear MIMO time-delay systems", *Automatica*, **43**, 31-43.

Ge, Z.M., Hsiao, C.L. and Chen, Y.S. (2005), "Nonlinear dynamics and chaos control for a time delay Duffing system", *Int. J. Nonlin. Sci. Numer.*, **6**(2), 187-199.

Greery, S.Mc., Soong, T.T. and Reinhorn, A.M. (1988), "An experimental study of time delay compensation in active structural control", *Proceedings of the Sixth International Modal Analysis Conference*, **1**, 733-739.

Hosek, M. and Olgac, N. (2002), "A single-step automatic tuning algorithm for the delayed resonator vibration absorber", *IEEE ASME Trans. Mechatron.*, **7**(2), 245-255.

Hu, H.Y. and Wang, Z.H. (2002), *Dynamics of Controlled Mechanical Systems with Delayed Feedback*, Springer-Verlag, Berlin.

Ikhouane, F., Hurtado, J.E. and Rodellar, J. (2007), "Variation of the hysteresis loop with the Bouc-Wen model parameters", *Nonlin. Dyn.*, **48**, 361-280.

Sun, Z.Q. (1989), *Theory and Application of Computer Control*, Tsinghua University Press, Beijing. (in Chinese)

Tian, E.G. and Peng, C. (2006), "Delay-dependent stability analysis and synthesis of uncertain T-S fuzzy systems with time-varying delay", *Fuzzy Sets Syst*., **157**, 544-559.
Wang, Z.H. and Hu, H.Y. (2006), "Stabilization of vibration systems via delayed state difference feedback", *J. Sound Vib*., **296**(1-2), 117-129.
Xiao, M. and Cao, J.D. (2007), "Bifurcation analysis and chaos control for Lu system with delayed feedback", *Int. J. Bifurcation Chaos*, **17**(12), 4309-4322.
Xu, J., Chung, K.W. and Chan, C.L. (2007), "An efficient method for studying weak resonant double Hopf bifurcation in nonlinear systems with delayed feedbacks", *SIAM J. Appl. Dyn. Syst*., **6**(1), 29-60.
Yang, J.N. and Liu, S.C. (1992), "Aseismic hybrid control of nonlinear and hysteretic structures II", *J. Eng. Mech.-ASCE*, **118**(7), 1441-1456.
Yuan, F. (2008), "Effects of delayed feedback control on stability in the cantilever pipe conveying fluid", Master thesis, Tongji University, Shanghai. (in Chinese)
Zhang, J.H., Shi, P. and Qiu, J.Q. (2008), "Robust stability criteria for uncertain neutral system with time delay and nonlinear uncertainties", *Chaos Solitons Fractals*, **38**, 160-167.